

The hydraulic bump: the surface signature of a plunging jet

M. Labousse¹ and J.W.M Bush^{2, a)}

¹*Institut Langevin, ESPCI ParisTech,
1 rue Jussieu 75005 Paris, France, EU*

²*Department of Mathematics, Massachusetts Institute of Technology,
77 Massachusetts Avenue, Cambridge, MA 02139, USA*

(Dated: 4 July 2021)

When a falling jet of fluid strikes a horizontal fluid layer, a hydraulic jump arises downstream of the point of impact provided a critical flow rate is exceeded. We here examine a phenomenon that arises below this jump threshold, a circular deflection of relatively small amplitude on the free surface, that we call the hydraulic bump. The form of the circular bump can be simply understood in terms of the underlying vortex structure and its height simply deduced with Bernoulli arguments. As the incoming flux increases, a breaking of axial symmetry leads to polygonal hydraulic bumps. The relation between this polygonal instability and that arising in the hydraulic jump is discussed. The coexistence of hydraulic jumps and bumps can give rise to striking nested structures with polygonal jumps bound within polygonal bumps. The absence of a pronounced surface signature on the hydraulic bump indicates the dominant influence of the subsurface vorticity on its instability.

PACS numbers: 47.20.Ma, 47.32.cd, 47.54.-r

Keywords: hydraulic jump, hydraulic bump, vortex ring, plunging jet, polygonal instability

^{a)}bush@math.mit.edu

I. INTRODUCTION

When a falling jet of fluid strikes a horizontal fluid layer, several flow regimes may arise. The most distinctive phenomenon, the hydraulic jump, arises above a critical flow rate, and consists of a large-amplitude increase in fluid depth at a critical distance from the site of jet impact (Figure 1 a). The circular hydraulic jump was first reported by Bélanger¹ and Rayleigh², and subsequently studied theoretically and experimentally by a number of investigators (see³⁻⁹ and references therein).

Bohr *et al.*⁶ and Watanabe *et al.*¹⁰ distinguished between circular hydraulic jumps of type I and II. The type I jump (see Figures 1 a, d) exhibits a single toroidal vortex downstream of the jump, henceforth “primary vortex”. As the outer depth is increased progressively, a separation of this vortex¹¹ is observed, giving rise to a surface roller, henceforth “secondary vortex” and a type II jump (Figure 1e,f). Yokoi *et al.*¹² presented a numerical investigation of the link between this vortex dynamics and the underlying pressure distribution in the type II jumps and remarked upon the importance of surface tension in the transition from type I to II. The type II jumps are further classified¹³ according to whether there is a substantial change in surface elevation downstream of the jump: if not, the jump is referred to as type IIa (Figure 1 b and e); if so, type IIb (Figure 1 c and f). Andersen *et al.*¹¹ and Bush *et al.*¹⁴ also reported the emergence of double jump structures in certain parameters regimes, wherein the free surface is marked by two discrete changes in depth.

Remarkably, in certain parameter regimes, the circular hydraulic jump becomes unstable to polygons (Figure 1b), a phenomenon first reported by Ellegaard^{15,16}, and subsequently examined by Bohr and coworkers^{11,17} and Bush *et al.*¹⁴. Watanabe *et al.*¹⁰ noted that the polygonal jumps arise exclusively with type II jumps, that is, when both primary and secondary vortices are present. Bush *et al.*¹⁴ highlighted the importance of surface tension in the polygonal instability of such jumps, suggesting that a modified Rayleigh-Plateau-like instability might be responsible. By considering a balance between the viscous stresses associated with the secondary vortex and the hydrostatic and curvature pressure, Martens *et al.*¹⁷ developed a theoretical model for the jump shape that yields polygons similar to those observed experimentally. When surface tension dominates, they demonstrate that

the wavelength of the instability is consistent with that of Rayleigh-Plateau. Nevertheless, they did not consider the potentially destabilizing influence of the pressure induced by the secondary roller vortex.

Plateau¹⁸ examined the capillary pinch-off of a fluid jet into droplets, a theoretical description of which was provided by Rayleigh¹⁹. This Rayleigh-Plateau instability was extended to the case of a rotating fluid jet by several investigators,^{20–22} who demonstrated that the destabilizing influence of surface tension is enhanced by fluid inertia. While vortex rings were initially thought to be indestructible^{23,24}, subsequent experimental, theoretical^{25–27} and numerical²⁸ studies indicate that they are unstable to azimuthal wavelength disturbances at high Reynolds numbers, resulting in polygonal forms. We here explore the possible relevance of a such instabilities to the stability of the hydraulic jump and bump.

Bush *et al.*¹⁴ briefly mentioned the emergence of polygonal forms in the absence of hydraulic jumps, when a jet plunges into a relatively deep fluid. Perrard *et al.*²⁹ recently reported that a heated toroidal fluid puddle bound in a circular channel and levitated via the Leidenfrost effect is also susceptible to polygonal instabilities. The axial symmetry breaking only arises in the presence of poloidal convection within the torus, again suggesting the importance of the vortical motion on the mechanism of instability.

We here report a phenomenon that occurs well below the hydraulic jump threshold, when the free surface is only weakly perturbed by the plunging jet. When the fluid layer is sufficiently deep, a small-amplitude circular deflection arises at the free surface, a phenomenon that we christen the hydraulic bump (Figure 1 g). As is the case for the hydraulic jump, as the incoming flux increases, the bump radius expands until a breaking of axial symmetry results in polygonal forms (Figure 1 h). In §II, we report the results of our experimental investigation, and describe the flows observed. We rationalize the radius of the bump via simple scaling laws. Finally, in §III we explore the connection between the polygonal instabilities on the hydraulic bump and their counterparts on the hydraulic jump.

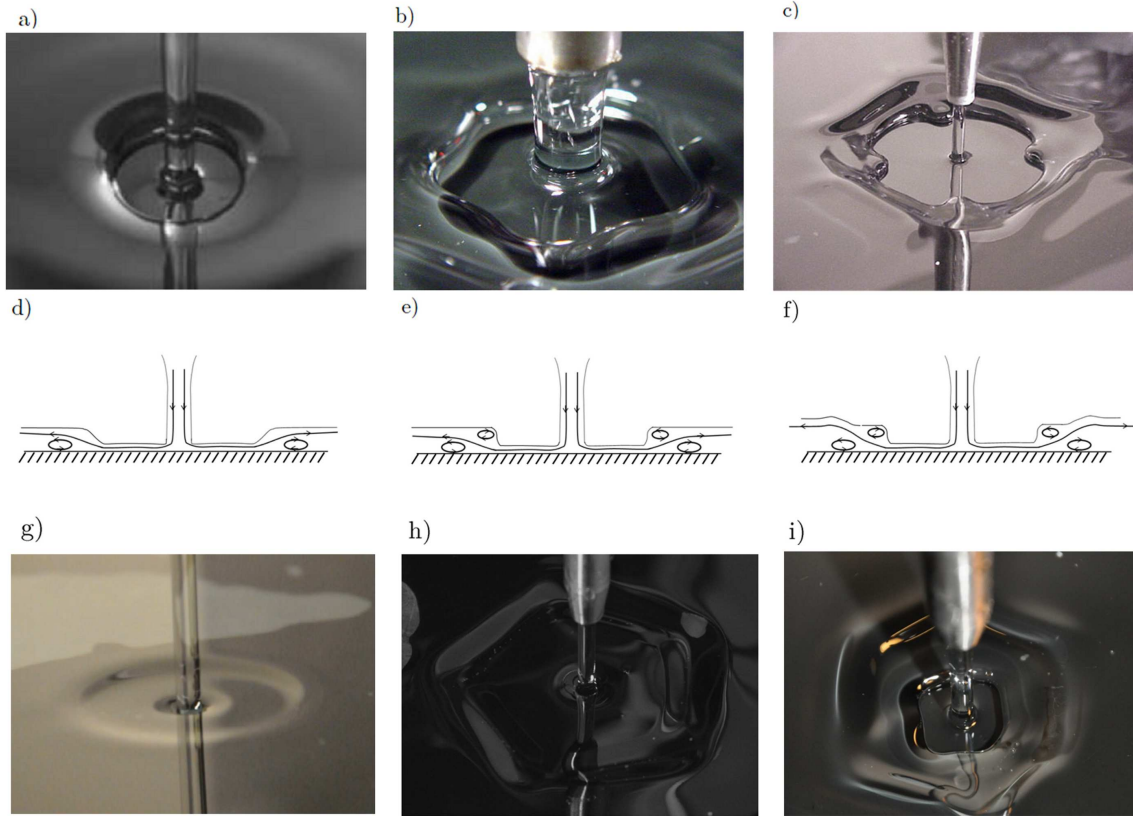


FIG. 1. a) The circular hydraulic jump⁸. b) A pentagonal hydraulic jump¹⁴. c) A clover-shaped jump inside a square bump¹⁴. d)-f) Schematics illustration of the hydraulic jump of type I d), IIa e) and IIb f). g) A circular hydraulic bump. h) A pentagonal hydraulic bump. i) A square hydraulic jump inside a hexagonal bump. a) Bush, J.W.M. and Aristoff, J.M., *J. Fluid Mech.* **489**, (2003) reproduced with permission. b) and c) Bush, J.W.M. and Aristoff, J.M. and Hosoi, A.E., *J. Fluid Mech.* **558**, (2006) reproduced with permission

II. EXPERIMENTS

The experimental apparatus is shown in figure 2. A glycerine-water solution with density ρ , kinematic viscosity ν , and a surface tension γ is pumped from the tank through a flow meter and a source nozzle of radius $R_n = 2.5$ mm. The resulting jet has a flux Q and a radius at impact r_j that differs from R_n , and varies weakly with flow rate and height in a manner detailed by Bush and Aristoff⁸. The jet impacts the center of a flat plate of radius $R_p = 16.8$ cm surrounded by an outer wall whose height can be adjusted in order to control

the outer fluid depth H . Radial gradations on the base plate indicate 0.5 cm increments. Special care is taken to level the plate by adjusting its three supports and measuring the level along two perpendicular directions. The plate is horizontal to within $\pm 0.1^\circ$. We note that the flow structure is extremely sensitive to the levelling of the plate; indeed, an inclination of $1 - 2^\circ$ completely destroys the polygonal bump and jump forms.

The working fluid is a glycerine-water solution with viscosity ranging from 58 to 96 cS. During the course of the experiments, water was added to compensate for evaporative losses. For the fluids considered, surface tension is roughly constant and equal to $68 \text{ mN}\cdot\text{m}^{-1}$. The average depth is determined by measuring the volume V_t above the impact plate, which is known with a precision $\pm \delta V_t = 2 \text{ ml}$. Typically, $V_t \simeq 500 \text{ ml}$ and $H \simeq 5 \text{ mm}$, so the error in depth $(\delta V_t H)/V_t \simeq 0.01 \text{ mm}$, is sufficient for our experiments and smaller than would arise from a direct measurement. We visualize the flow structure by injecting submillimetric bubbles into the jet inlet with a syringe and taking photos that yield streak images of the bubble circulation. In passing through the pump and the flowmeter, these bubbles are generally fractured into microbubbles that do not appreciably perturb the flow. We denote by R_{bump} the bump radius, δH its height and H_{int} the height just upstream of the bump. We denote the fluid velocity by \mathbf{v} and its speed by v . This suggests the introduction of the Reynolds number $Re = v_j H/\nu$, with the jet speed $v_j = Q/(\pi R_n^2)$ being evaluated at the nozzle output, and a local Weber number $We = \rho Q^2/(\gamma \pi^2 H R^2)$, with R being the radius of the jump or the bump.

Figure 3 illustrates the evolution of the flow generated by a plunging jet as the flux increases and the fluid depth H is held constant. We note that the flux of the impacting jet is not sufficiently high to entrain air^{30,31}. Initially (Figure 3a), the plunging jet induces a slight circular deflection, perceptible only from an oblique angle, and the subsurface flow is predominantly radial. At a critical flow rate, a recirculation eddy emerges, and with it the hydraulic bump (figure 3b). We note that this subsurface recirculation eddy, or primary vortex, is accompanied by a small corotating secondary vortex with a surface signature that corresponds to the bump. As the flux increases, the bump increases in both amplitude and radius. At a critical flux, azimuthal instabilities develop along its perimeter (figure 3c), giving rise to a stable polygonal bump (figure 3d). As the bump has a very modest surface

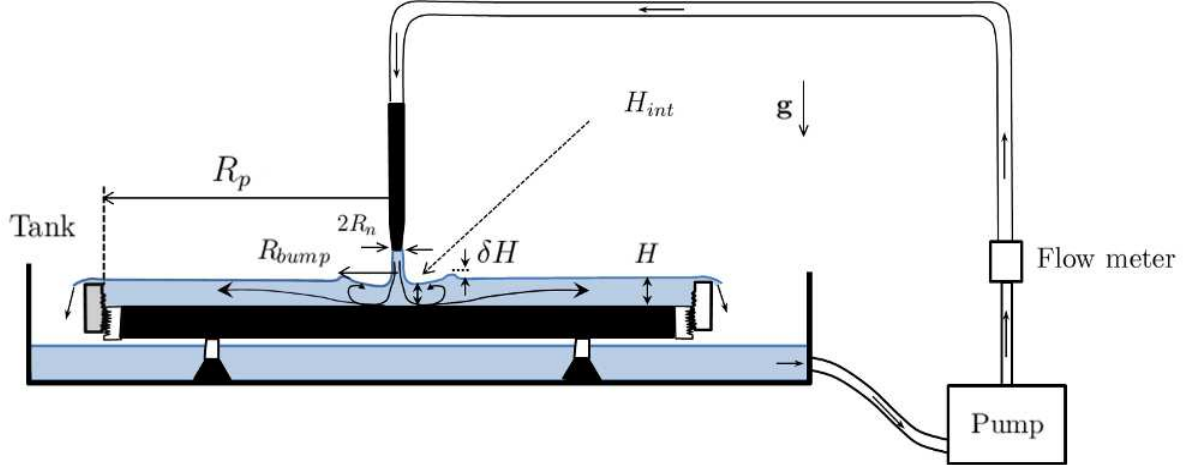


FIG. 2. Schematic illustration of the experimental apparatus and the hydraulic bump

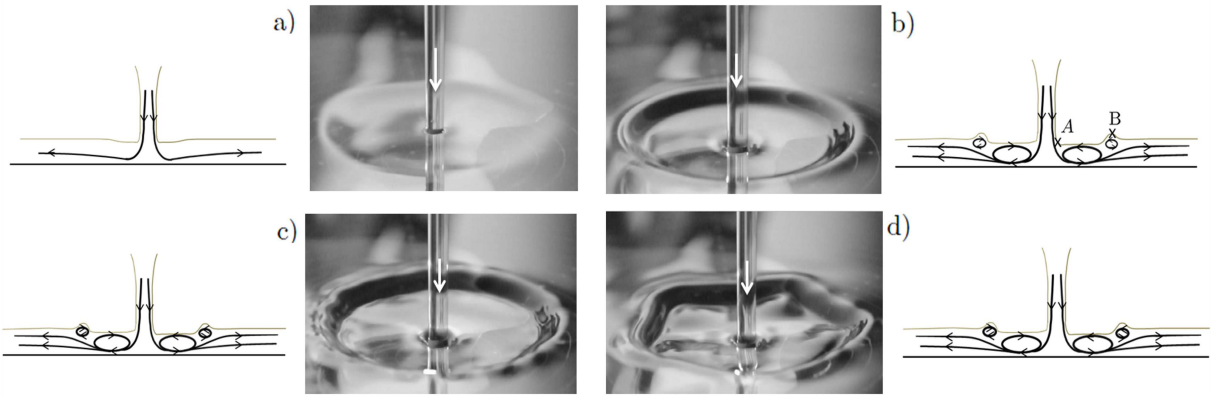


FIG. 3. Evolution of the flow generated by a plunging jet with increasing Q . Here, $\nu = 68$ cS, $H = 6.65$ mm. Accompanying schematic illustrations of the subsurface flows induced from streak images are displayed. a) Below the bump transition ($Q = 6.6$ ml.s $^{-1}$). b) The circular bump is marked by a toroidal vortex ($Q = 13.3$ ml.s $^{-1}$). c-d) At a critical flux ($Q = 18.3$ ml.s $^{-1}$), the bump becomes susceptible to instabilities that result in a polygonal form.

signature, much less than the jump, we infer that the subsurface vortical structure is critical in its instability.

The height and radius of the circular bump are readily rationalized via scaling arguments. We consider a point A at the surface near the plunging jet and a point B on the bump (see Figure 3b). We denote by δH the amplitude of the bump. Since B can be considered as a

stagnation point and since curvature pressures are expected to be negligible with respect to the hydrostatic pressure within the bump, Bernoulli's Theorem dictates that $v_A^2/2 - g\delta H = \text{const.}$, so we expect that $\delta H = c_1 v_A^2/2g$ with $v_A \simeq Q/(2\pi R_n H)$. Figure 4a illustrates the dependence of $2g\delta H$ on $Q^2/(4\pi^2 R_n^2 H^2)$ over the parameter range in which circular bumps arise. This simple scaling is roughly validated, and a proportionality constant of $c_1 = 0.41$ is indicated.

Figure 4b illustrates the dependence of the bump radius R_{bump} on the flux Q and the kinematic viscosity ν of the fluid over the range of Weber and Reynolds numbers in which circular bumps emerge. The characteristic radius of the inner vortex can be deduced by considering the azimuthal component of the vorticity equation. In a steady state, the balance of convection and diffusion of vorticity ω requires that $(\mathbf{v} \cdot \nabla)\omega \sim \nu \Delta \omega$. The typical scale of the vertical flow is H_{int} , the inner depth. Thus, balancing $(\mathbf{v} \cdot \nabla)\omega \sim v\omega/H_{int}$ and $\nu \Delta \omega \sim \nu\omega/H_{int}^2$ and using $v \sim Q/(2\pi R_{bump} H_{int})$ indicates that $R_{bump} = c_2 Q/(2\pi\nu)$. Figure 4b lends support to this scaling argument, and suggests a proportionality coefficient of $c_2 = 2.5$.

As illustrated in Figure 1c and 1i, non-circular bumps may also arise downstream of polygonal hydraulic jumps. Similar nested jump-bump structures have been reported by Andersen *et al.*¹¹ and Bush *et al.*¹⁴. We note that the number of sides of the outer bump and inner jump polygons are not necessarily the same. Figure 1i illustrates a square jump within a pentagonal bump.

Figure 5 indicates where the various flow structures, specifically circular and polygonal hydraulic jumps and bumps, arise in the (We, Re) plane. In addition to our new data, this regime diagram includes data from Bush *et al.*¹⁴, with due care given to their different definitions of the Weber and Reynolds numbers. In our experiments, as Q is increased, the data necessarily traverses a path on the regime diagram along which $Re \propto \sqrt{We}$. The dependence of the flow structure on viscosity was examined by progressively diluting the solution. We note that in sufficiently dilute solutions, the polygonal forms are unstable owing to the onset of turbulence. Viscosity is thus critical in the suppression of turbulence, and the sustenance of stable jumps, which only arise in the moderate Reynolds number range: $Re \simeq 20 - 100$.

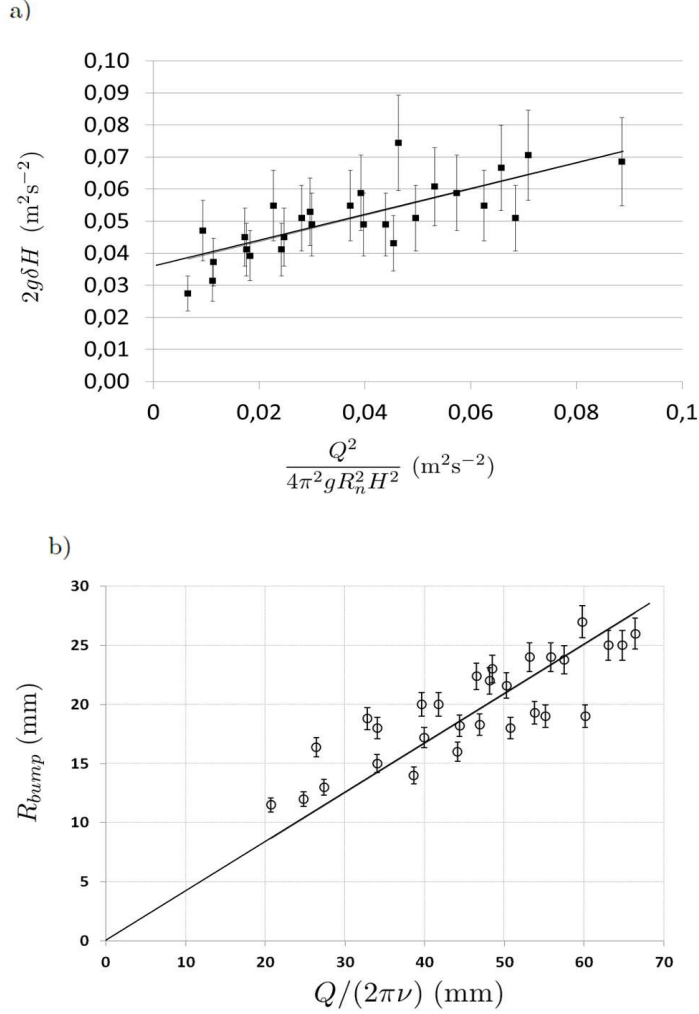


FIG. 4. a) The dependence of the circular bump amplitude, $2g\delta H$ (m^2s^{-2}), on $v_A^2 = Q^2/(4\pi^2 R_n^2 H^2)$ (m^2s^{-2}). The uncertainties on δH are approximately 20 %. b) The observed dependence of the bump radius R_{bump} (mm) on $Q/(2\pi\nu)$ (mm). The bumps are formed with glycerine-water solutions, with viscosity ranging from 58 to 96 cS

III. CONCLUSION

We have characterized the flows generated by a laminar fluid jet plunging into a bath of the same fluid, giving particular attention to the accompanying subsurface vortex structure and its instability. We have reported and rationalized a new interfacial structure, the circular hydraulic bump, the small surface deflection that arises prior to the onset of the hydraulic jump. The bump coincides with the stagnation point associated with the sub-

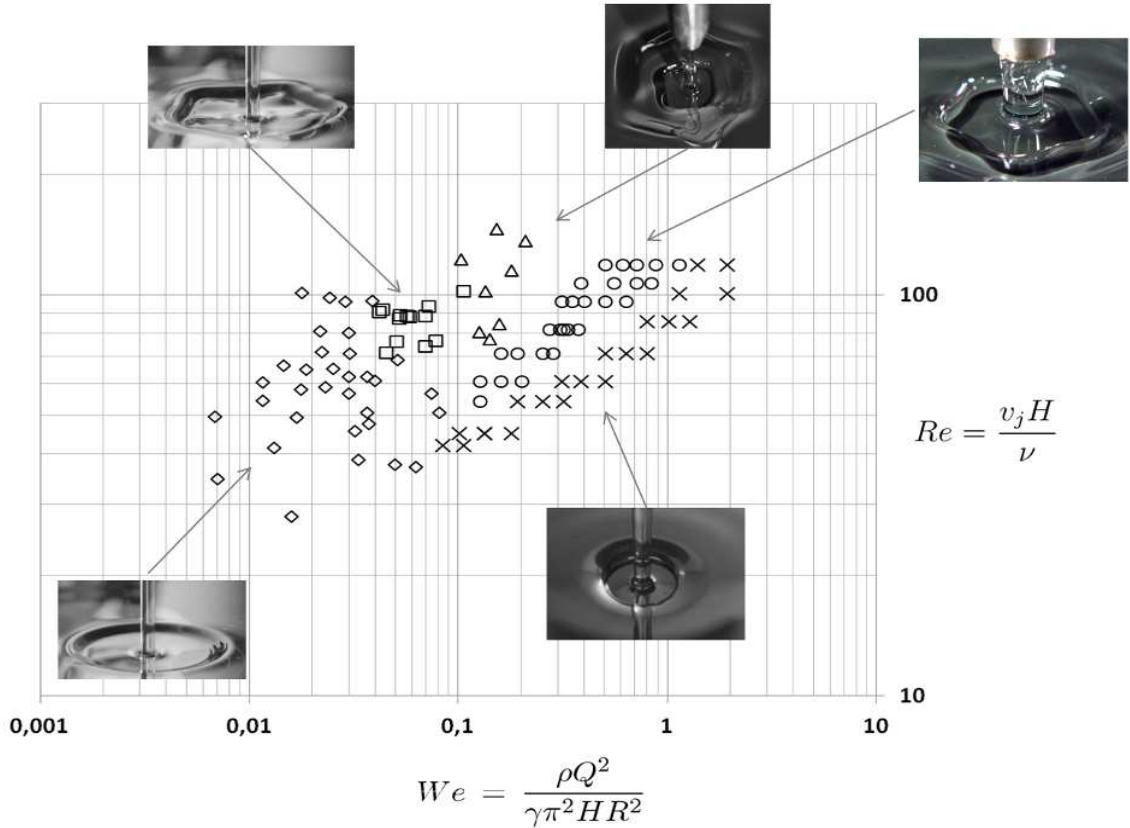


FIG. 5. The dependence of the flow structure on Reynolds $Re = (v_j H)/\nu$ and Weber number $We = \rho Q^2 / (\gamma \pi^2 H R^2)$, where $v_j = Q / (2\pi R_n)$ is the jet speed, and R the radius of the bump or jump. \diamond : circular bumps observed for viscosities in the range of $\nu = 58 - 96$ cS. \square : polygonal bumps ($\nu = 58 - 96$ cS) with number of sides ranging from 5 to 10. \triangle : the double jump structure for which a polygonal jump is enclosed by a polygonal bump. \times : circular type I jumps ($\nu = 10$ cS, from Bush *et al.*¹⁴). \circ : polygonal jumps with 3 to 10 sides ($\nu = 10$ cS, data from Bush *et al.*¹⁴). Bush, J.W.M. and Aristoff, J.M. and Hosoi, A.E., *J. Fluid Mech.* **558**, (2006) used with permission

surface vortex generated by the plunging jet and consists of a small toroidal vortex with a surface signature. Simple scaling arguments have allowed us to rationalize both the radius and amplitude of the bump.

We have also reported that, as the flux increases, the circular bump goes unstable to a polygonal form reminiscent of that arising in the hydraulic jump¹⁴. We note that the

polygonal instabilities of both the jump and bump are associated with a toroidal vortex with a surface signature. Since the bump has a relatively small surface signature, we expect its accompanying subsurface vorticity to provide the dominant mechanism for its instability. This surface vortex instability mechanism, and its relation to the hydraulic bump, the hydraulic jump, and the toroidal Leidenfrost vortex²⁹, will be the subject of a theoretical investigation to be reported elsewhere.

ACKNOWLEDGMENTS

The authors acknowledge the generous financial support of the National Science Foundation through grant number DMS-0907955. M.L. is grateful to José Bico, Marc Fermigier from the PMMH laboratory and “La société des Amis de l’ESPCI ParisTech” for funding this partnership work between the ESPCI ParisTech and MIT. We would like to thank Yves Couder, Stéphane Perrard and Laurent Limat at the MSC laboratory for valuable discussions.

REFERENCES

- ¹J. Bélanger, “Notes sur l’hydraulique,” École Royale des Ponts et Chaussées (1841).
- ²Lord Rayleigh, “On the theory of long waves and bores,” Proc. R. Soc. Lond. A **90**, 324–328 (1914).
- ³I. Tani, “Water jump in the boundary layer,” J. Phys. Soc. Jpn. **4**, 212–215 (1949).
- ⁴E. Watson, “The radial spread of a liquid jet over a horizontal plane,” J. Fluid Mech. **20**, 481–499 (1964).
- ⁵T. Bohr, P. Dimon, and V. Putkaradze, “Shallow-water approach to the circular hydraulic jump,” J. Fluid Mech. **254**, 635–648 (1993).
- ⁶T. Bohr, C. Ellegaard, A.E. Hansen, and A. Haaning, “Hydraulic jumps, flow separation and wave breaking: An experimental study,” Physica B **228**, 1–10 (1996).
- ⁷T. Bohr, V. Putkaradze, and S. Watanabe, “Averaging theory for the structure of hydraulic jumps and separation in laminar free-surface flows,” Phys. Rev. Lett. **79**, 1038–1041 (1997).

- ⁸J.W.M. Bush and J.M. Aristoff, “The influence of surface tension on the circular hydraulic jump,” *J. Fluid Mech.* **489**, 229–238 (2003).
- ⁹A.R. Kasimov, “A stationary circular hydraulic jump, the limits of its existence and its gasdynamic analogue,” *J. Fluid Mech.* **601**, 189–198 (2008).
- ¹⁰S. Watanabe, V. Putkaradze, and T. Bohr, “Integral methods for shallow free-surface flows with separation,” *J. Fluid Mech.* **480**, 233–265 (2003).
- ¹¹A. Andersen, T. Bohr, and T. Schnipper, “Separation vortices and pattern formation,” *Theor. Comput. Fluid Dyn.* **24**, 329–334 (2009).
- ¹²K. Yokoi and F. Xiao, “Mechanism of structure formation in circular hydraulic jumps: numerical studies of strongly deformed free-surface shallow flows,” *Physica D* **161**, 202–219 (2002).
- ¹³X. Liu and J.H. Lienhard V, “The hydraulic jump in circular jet impingement and in other thin liquid films,” *Exp. Fluids* **15**, 108–116 (1993).
- ¹⁴J.W.M. Bush, J.M. Aristoff, and A.E. Hosoi, “An experimental investigation of the stability of the circular hydraulic jump,” *J. Fluid Mech.* **558**, 33–52 (2006).
- ¹⁵C. Ellegaard, A. Hansen, A. Haaning, K. Hansen, A. Marcussen, T. Bohr, J. Hansen, and S. Watanabe, “Creating corners in kitchen sinks,” *Nature* **392**, 767–768 (1998).
- ¹⁶C. Ellegaard, A.E. Hansen, A. Haaning, K. Hansen, A. Marcussen, T. Bohr, J.L. Hansen, and S. Watanabe, “Cover illustration: polygonal hydraulic jumps,” *Nonlinearity* **12**, 1–7 (1999).
- ¹⁷E. Martens, S. Watanabe, and T. Bohr, “Model for polygonal hydraulic jumps,” *Phys. Rev. E* **85** (2012).
- ¹⁸J. Plateau, “Experimental and theoretical statics of liquids subject to molecular forces only,” *Gauthier-Villars, Paris* **1**, 4–13(1873).
- ¹⁹Lord Rayleigh, “On the instability of jets,” *Proc. Lond. M. Soc.* **10** (1878).
- ²⁰L. M. Hocking and D. H. Michael, “The stability of a column of rotating liquid,” *Matematika* **6**, 25–32 (1959).
- ²¹T.J. Pedley, “The stability of rotating flows with a cylindrical free surface,” *J. Fluid Mech.* **30**, 127–147 (1967).
- ²²J. Kubitschek and P. Weidman, “The effect of viscosity on the stability of a uniformly rotating liquid column in zero gravity,” *J. Fluid Mech.* **572**, 261–286 (2007).
- ²³Sir W. Thomson, “On vortex atoms,” *Phil. Mag.* **34**, 15 – 24 (1867).

- ²⁴J.J. Thomson, “A treatise on the motion of vortex ring,” Macmillan, London (1883).
- ²⁵S.E. Widnall and C.Y. Tsai, “The instability of the thin vortex ring of constant vorticity,” *Phil. Trans. R. Soc. Lond. A* **287**, 273–305 (1977).
- ²⁶T. Maxworthy, “Some experimental studies of vortex rings,” *J. Fluid Mech.* **81**, 465 – 495 (1977).
- ²⁷P. Saffman, “The number of waves on unstable vortex rings,” *J. Fluid Mech.* **84**, 625 – 639 (1978).
- ²⁸O.M. Knio and A.F. Ghoniem, “Numerical study of a three-dimensional vortex method,” *J. Comput. Phys.* **86**, 75–106 (1990).
- ²⁹S. Perrard, Y. Couder, E. Fort, and L. Limat, “Leidenfrost levitated liquid tori,” *Europhys. Lett.* **100**, 54006 (2012).
- ³⁰A.K Biń, “Gas entrainment by plunging liquid jets,” *Chem. Eng. Sci.* **48**, 3585 – 3630 (1993).
- ³¹E. Lorenceau, D. Quéré, and J. Eggers, “Air entrainment by a viscous jet plunging into a bath,” *Phys. Rev. Lett.* **93** (2004).